Quantification of Global MicroRNA Abundance by Selective Isotachophoresis

ARTICLE *in* ANALYTICAL CHEMISTRY · NOVEMBER 2010

Impact Factor: 5.64 · DOI: 10.1021/ac102496m · Source: PubMed

4 AUTHORS, INCLUDING:

Alexandre Persat
Princeton University
17 PUBLICATIONS **244** CITATIONS
SEE PROFILE

Juan G Santiago
Stanford University
307 PUBLICATIONS **10,549** CITATIONS
SEE PROFILE

Quantification of Global MicroRNA Abundance by Selective Isotachophoresis

Alexandre Persat,[†] Raghu R. Chivukula,[‡,§] Joshua T. Mendell,[‡,§] and Juan G. Santiago*[,†]

Department of Mechanical Engineering, Stanford University, Stanford, California 94305, United States, Johns Hopkins University, School of Medicine, Baltimore, Maryland 21205, United States, and Howard Hughes Medical Institute, Chevy Chase, Maryland 20815, United States

We here present and demonstrate a novel technique based on isotachophoresis (ITP) for the quantification of global microRNA (miRNA) abundance in total RNA. We leverage the selectivity of ITP to concentrate miRNA and exclude longer RNA molecules from the focused zone. We designed a novel ITP strategy where we initially establish three contiguous zones of sieving polymer, electrolyte, and denaturant concentrations. This allows for successive preconcentration, selection, and detection of miRNA. We optimized chemistry in each zone for high sensitivity and exquisite selectivity for miRNA. This technique allows for the measurement of the total miRNA content in a sample and its comparison between different cell types and tissues. We demonstrated and validated the efficacy of this technique by comparing global miRNA abundance in subconfluent and confluent cell cultures.

MicroRNAs (miRNAs) are a class of 18−24 nucleotide (nt) noncoding RNAs that regulate gene expression via sequence-specific interactions with mRNAs.[1] Several hundred miRNAs are encoded in the human genome and dozens have now been shown to regulate a diverse variety of cellular processes, both in normal physiology and in disease.[2]

miRNAs are liberated from long, RNA Polymerase II transcribed precursors by a series of sequential endonuclease-mediated cleavage events and are turned over by mechanisms that remain poorly characterized.[1] Evidence is now accumulating that miRNA biogenesis is subject to regulation, allowing cells to selectively control the production of these small RNAs and thereby titrate their regulatory activity. For example, recent studies have demonstrated that the expression of many miRNAs increases during early embryonic development.[3] Conversely, miRNA abundance is globally reduced in a wide variety of human cancers.[2] Moreover, it was recently demonstrated that global miRNA abundance increases as cells are grown to high density in culture.[4] These findings highlight the need for accurate, high-throughput methods to quantify the global abundance of miRNAs in total RNA samples derived from diverse sources. Such methodology would greatly facilitate investigation of the mechanisms that regulate miRNA biogenesis and the settings in which these pathways operate.

To investigate the correlation between miRNA expression and cell density, Hwang et al.[4] used microarrays and Northern blots to analyze RNA samples from various culture conditions. These measurements require large amounts of sample, do not necessarily include all miRNAs, and do not allow for absolute quantification. A commercial electrophoresis system for quantification of small RNAs was reported recently.[5] By accounting for RNA longer than the range of miRNA (up to 40 nt), this instrument overestimates miRNA abundance.[6] Moreover, the measurement may suffer the same effect from the dispersion of longer RNA (in particular abundant tRNA) into the range of measurement. We here demonstrate a technique which allows fast, accurate, and absolute measurement of global miRNA levels from small amounts of total RNA using highly selective multistage on-chip ITP.

ITP is an electrophoretic focusing technique which leverages strong electric field gradients to focus and separate ions based on their electrophoretic mobilities (cf. Figure S1 in the Supporting Information).[7,8] In ITP, we select trailing and leading electrolytes (TE and LE) to have, respectively, smaller and larger electrophoretic mobility than the target ion(s) of interest. In ITP, species with mobilities smaller than the TE (or greater than LE) will not focus. We have used this feature of ITP to extract PCR-compatible genomic DNA samples from whole blood[9] and to isolate short nucleic acids from the cell lysate.[10] In this work, we purified total RNA using a standard technique, as described below. Then, we diluted this total RNA in the TE. We use the selectivity of ITP to focus exclusively (mature) miRNA from this total RNA while

* To whom correspondence should be addressed. E-mail: juan.santiago@stanford.edu.

[†] Stanford University.

[‡] Johns Hopkins University.

[§] Howard Hughes Medical Institute.

(1) He, L.; Hannon, G. J. *Nat. Rev. Genet.* **2004**, *5*, 522–531.

(2) Lu, J.; Getz, G.; Miska, E. A.; Alvarez-Saavedra, E.; Lamb, J.; Peck, D.; Sweet-Cordero, A.; Ebet, B. L.; Mak, R. H.; Ferrando, A. A.; Downing, J. R.; Jacks, T.; Horvitz, H. R.; Golub, T. R. *Nature* **2005**, *435*, 834–838.

(3) Thomson, J. M.; Newman, M.; Parker, J. S.; Morin-Kensicki, E. M.; Wright, T.; Hammond, S. M. *Genes Dev.* **2006**, *20*, 2202–2207.

(4) Hwang, H. W.; Wentzel, E. A.; Mendell, J. T. *Proc. Natl. Acad. Sci. U.S.A.* **2009**, *106*, 7016–7021.

(5) Masotti, A.; Caputo, V.; Da Sacco, L.; Pizzuti, A.; Dallapiccola, B.; Bottazzo, G. F. *J. Biomed. Biotechnol.* **2009**; 659028.

(6) Becker, C.; Hammerle-Fickinger, A.; Riedmaier, I.; Pfaffl, M. W. *Methods* **2010**, *50*, 237–243.

(7) Khurana, T. K.; Santiago, J. G. *Anal. Chem.* **2008**, *80*, 6300–6307.

(8) Everaerts, F. M.; Beckers, J. L.; Verheggen, T. P. E. M. *Isotachophoresis: Theory, Instrumentation, and Applications*; Elsevier Scientific Pub. Co.: Amsterdam, The Netherlands, 1976.

(9) Persat, A.; Marshall, L. A.; Santiago, J. G. *Anal. Chem.* **2009**, *81*, 9507–9511.

(10) Schoch, R. B.; Ronaghi, M.; Santiago, J. G. *Lab Chip* **2009**, *9*, 2145–2152.

10.1021/ac102496m

leaving longer RNA molecules unfocused. We then quantify the amount of focused sample by fluorescence to obtain a measurement of the global amount of miRNA in the sample of interest. In separate ITP experiments, we build a calibration curve with known amounts of miRNA, allowing for absolute miRNA quantitation.

High selectivity in ITP can be achieved by tuning the concentration of sieving matrix in the LE such that the mobility of miRNA is only slightly larger than the TE mobility. However, this implies that unfocused miRNA in the TE migrates at nearly the same speed as the ITP interface; thus resulting in slow focusing rate and a low level of preconcentration and sensitivity.[7] Also, denaturing conditions are required for high selectivity but can interfere with quantum yield and affinity of fluorescent reporters. To achieve both high selectivity and high sensitivity, we have designed an ITP assay with multiple zones of varying sieving matrix and denaturant concentrations. These are established using three initial LE zones. We know of no other work using such a multistage sieving matrix ITP. We first describe our assay qualitatively and then describe the injection protocol and the specific chemistry of the LE zones and TE.

In the microfluidic chip, we establish three initial LE zones arranged in series along the separation channel and suppress the electroosmotic flow. Initial LE zones 1, 2, and 3 have different initial concentrations of chloride (leading ion) C_{LI}, polymer sieving matrix C_p, and denaturant C_d. Our sample is initially mixed uniformly with TE and dispensed into the TE reservoir. Figure 1 depicts the sample migration through the three zones. Sample travels behind LE ions but through three stationary regions of sieving matrix and denaturant (each electrically neutral) established by the initial condition.

The initial zone LE1 has low C_p, resulting in miRNA mobility significantly larger than that of the TE and increased miRNA flux to the ITP interface. High C_{LI} in LE1 also enhances preconcentration.[11] The initial zone LE2 has high C_p for selective focusing of miRNA and defocusing of longer RNA. This transition is shown in Figure 1a, where the narrow green band represents miRNA and the dispersed orange band is longer RNA. The spatiotemporal diagram of Figure 1b is an experimental demonstration of this process, where we focused 22 nt and 60 nt long RNA in zone LE1 and selectively defocused the 60 nt long RNA in zone LE2. The spatiotemporal plot shown is measured experimentally by integrating the image intensity along the channel width (perpendicular to the axis) and plotting this integrated image data versus distance and time. This experiment illustrates the combination of ITP preconcentration in LE1 with the selectivity of ITP in LE2 shown in Figure 1a.

The mobility of RNA is strongly affected by its secondary structure, requiring use of denaturing agents.[12] We use urea in the LE1 and LE2 zones to increase separation resolution for greater accuracy, but this significantly decreases fluorescence of the RNA stain. Consequently, we use reduced denaturing conditions (low C_d) in LE3, so this last section acts as a detection zone. An experimental demonstration of the transition between the LE2 and LE3 zones is shown in the spatiotemporal diagram

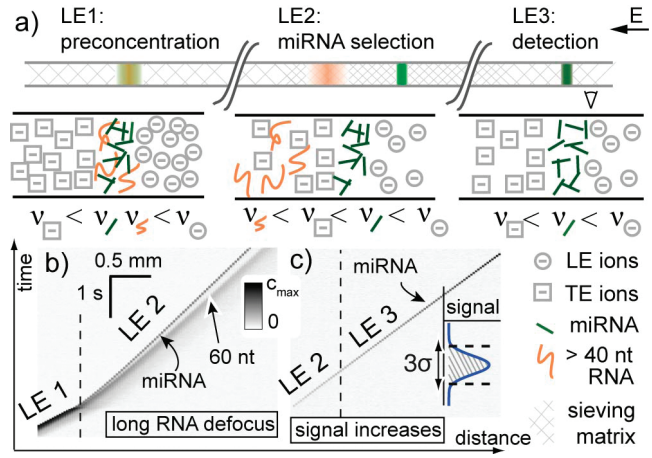

Figure 1. Schematic (a) and experimental demonstration (b and c) of three-zone ITP for the selective focusing and quantification of miRNA. In part a, LE1 (left) contains high LE concentration and low concentration of sieving polymer matrix (depicted by widely space cross hatching) to allow for a high flux of miRNA to the ITP interface. LE2 (middle) contains a high concentration sieving matrix to defocus 40 nt or longer RNA while keeping miRNA focused. The top right arrow shows the direction of the electric field, *E*. An experimental demonstration of the defocusing is shown in the spatiotemporal diagram (b) showing a measured channel-width-averaged fluorescence intensity data (inverted gray scale) versus axial channel distance and time. In this experiment, a mixture of 22 nt and 60 nt long RNA focus in LE1 but only the 22 nt RNA remains focused in LE2. In part c, we show an experimental demonstration of the transition between LE2 and LE3. The LE3 zone (right) has reduced denaturant concentration enabling higher fluorescence for sensitive quantification of the selectively focused miRNA. The latter experiment's measured spatiotemporal diagram shows transition of a 22 nt RNA focused peak (line crossing the figure) from low fluorescence in LE2 (light gray line in the bottom left) to significantly larger fluorescence in LE3 (darkening line). In this experiment, fluorescence intensity increases approximately 8-fold. We acquire data 8 mm into the LE3 zone by integrating signal over 3.0 standard deviations, as illustrated on the signal peak in the bottom right.

of Figure 1c, where the 22 nt long RNA remains focused (light gray streak) but fluorescence signal significantly increases in the LE3 zone (darkening gray streak). This experiment illustrates the transition from zones LE2 to LE3 shown in Figure 1a.

METHODS

For control experiments, we used HPLC purified synthetic miRNAs, 40 nt and 60 nt long RNA (Integrated DNA Technologies, Coralville, IA; the 22 nt long miR-126 complement was synthesized at the Stanford PAN facility) whose sequences are given in Table s1 in the Supporting Information, and yeast tRNA (Invitrogen, Carlsbad, CA). We used an equimolar mixture of 735 synthetic miRNAs (mirVana miRNA reference panel v9.1, Ambion, Austin, TX) to generate the calibration curves of Figure 5a. For the validation and demonstration of quantification assay (Figure 5b), we purified RNA from subconfluent and confluent HeLa and Hepa1-6 cells using Trizol (Invitrogen; see Hwang et al. for description of the culture method[4]). We measured total RNA concentration with a NanoDrop 2000 spectrophotometer (Thermo Scientific, Rockford, IL) and diluted all stock solutions to 0.5 $\mu g \cdot \mu L^{-1}$ before storage at −80 °C. Before running each ITP experiment, we diluted the specified RNA sample into 100 μL of TE. This sample/TE mixture was then denatured in a 70 °C

(11) Bocek, P.; Deml, M.; Janak, J. *J. Chromatogr., A* **1978**, *156*, 323–326.
(12) Todorov, T. I.; Yamaguchi, Y.; Morris, M. D. *Anal. Chem.* **2003**, *75*, 1837–1843.

Table 1. Detailed Composition of LE1, LE2, and LE3

	Tris HCl, pH = 8.0 (mM)	PVP (MW = 1 000 000)	urea (M)	SYTO RNASelect (nM)
LE1	100	0.5% w/v	7	500
LE2	20	5.5% w/v (varies in Figure 2)	7	500
LE3	20	3% w/v	2	500

water bath for 5 min to ensure full disruption of RNA secondary structures and placed on ice.

The LEs all contain DNase, RNase free Tris hydrochloride (pH = 8.0, Invitrogen, Carlsbad, CA), urea (EMD Biosciences, Gibbstown, NJ), polyvinylpyrrolidone (PVP, MW = 1 000 000, Polysciences Inc., Warrington, PA). LE1 and LE2 were prepared from a stock solution of 8 M urea and 6.8% w/v PVP. We provide details of concentrations for each LE in Table 1. For RNA quantitation, we used 500 nM SYTO RNaselect dye (Invitrogen), except for the spatiotemporal diagrams of Figure 1 where we used 1x SYBR Green II (Invitrogen). The TE is a solution of 92.5% v/v formamide (Invitrogen) containing 5 mM Tris (Sigma-Aldrich, Saint Louis, MO) and 2.5 mM caproic acid (Fluka, Milwaukee, WI). All solutions were made using DNase RNase free water (Gibco, Carlsbad, CA).

We performed the ITP experiment in a microchip with a 8 cm long main microchannel with multiple T-junctions and side channels (cf. Figure 2). We detail the injection procedure to create the initial multistage LE train in the Supporting Information (Table s2). Briefly, three LE zones are established by applying vacuum at reservoirs 3 and 7 (in Figure 2). This effectively fills the microchannel segment 1-A with LE1 (gray), A−B with LE2 (red) and B−8 with LE3 (green). After rinsing the TE reservoir, we add the sample/TE and apply the electric potential difference between reservoirs 1 and 8.

Details of our confocal optical setup and a schematic of the experimental setup (Figure s2) are provided in Supporting Information. Briefly, we performed visualizations on an inverted epifluorescence microscope equipped with a diode laser and measured fluorescence intensity using a photomultiplier tube 8 mm into the LE3 zone. We calculated fluorescence intensity by integrating the ITP zone signal peak as shown in the signal peak in the inset of Figure 1c.

To perform exquisitely selective miRNA focusing, we first chose a TE whose mobility was smaller than the mobility of short

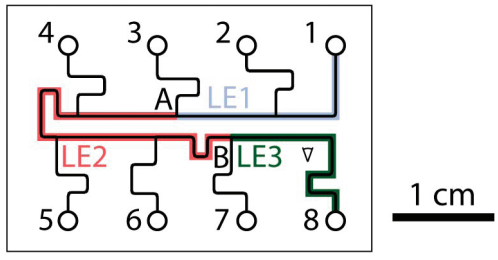

Figure 2. Design of the caliper NS260 borosilicate glass microchip. Before each experiment, we fill the microchannels with LE1 (gray), LE2 (red), and LE3 (green) according the sequence described in Table s2 in the Supporting Information. Channel width is not to scale. The three LE zones are highlighted for clarity. The detector is placed 8 mm into the LE3 zone.

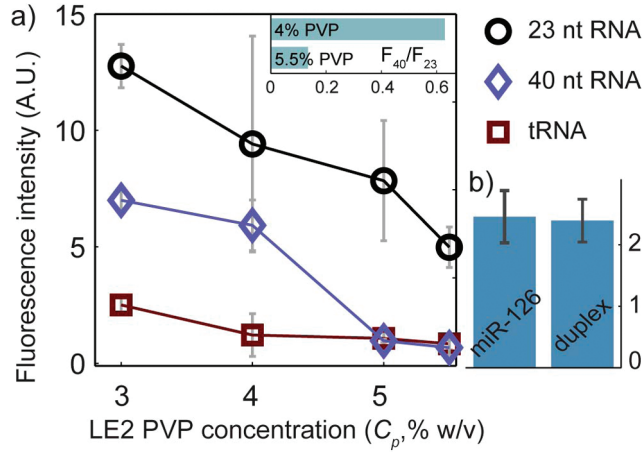

Figure 3. Demonstration of selectivity of miRNA focusing (a) and effect of potential base pairing on miRNA fluorescence in ITP (b). We performed ITP using 23 nt and 40 nt long RNA and tRNA dissolved in the TE. We report total intensity in the focused zone for increasing polymer concentration in LE2. All RNA focus at 3% w/v PVP. At 5% w/v and above, we observe significant focusing of the 23 nt RNA while both 40 nt and tRNA are rejected. The inset shows a horizontal bar chart of 40-nt-to-23-nt signal ratio (F_{40}/F_{23}). At 4% w/v PVP, F_{40}/F_{23} is greater than 0.6 but drops down to 0.12 at 5.5% w/v. We chose to use 5.5% w/v PVP in LE2 for selective focusing of miRNA. We also verified that potential base pairing of miRNA does not affect fluorescence. In part b, we show results of selective focusing of miR-126 (5 pg·μL^{-1} in TE) and of an equimolar mixture of miR-126 and its complementary RNA (each at 2.5 pg·μL^{-1}). There is no significant difference between fluorescence of miR-126 and of the duplex, showing no bias due to base pairing. Uncertainty bars represent 95% confidence intervals.

nucleic acids (for zero C_p)[13] and chose nominal values for C_p in LE1 and LE2. We then performed a series of experiments with increasing C_p (and decreasing local RNA mobility[14]) in LE2. Such titration allowed tuning of the cutoff focusing length (length below which RNA focuses).

RESULTS AND DISCUSSION

In Figure 3a, we show results of three sets of titration experiments using 23 and 40 nt synthetic oligoribonucleotides and yeast tRNA. We used a 40 nt long synthetic oligo to simulate RNA longer than miRNA and tRNA (80 nt in average[15]) to verify that highly abundant short RNAs with strong secondary structures do not interfere with our measurement. The titration aimed at finding the C_p to focus miRNA but reject 40 mer and tRNA. For all three RNAs, the amount of focused RNA gradually decreased with increasing PVP initial concentration in LE2. This is consistent with a global decrease of nucleic acid electrophoretic mobility and associated decreased flux of RNA to the ITP interface.[7] At 3% w/v PVP, there was significant focusing of all three RNA types. Increasing PVP concentration to 4% w/v resulted in defocusing of tRNA, shown by the drop in tRNA signal to the baseline value. 40 nt RNA was rejected at 5% w/v PVP. Meanwhile, the amount of 23 nt long RNA remained

(13) Stellwagen, N. C.; Gelfi, C.; Righetti, P. G. *Biopolymers* **1997**, *42*, 687–703.
(14) Barron, A. E.; Sunada, W. M.; Blanch, H. W. *Electrophoresis* **1996**, *17*, 744–757.
(15) Alberts, B. *Molecular Biology of the Cell*, reference ed.; Garland Science: New York, 2008.

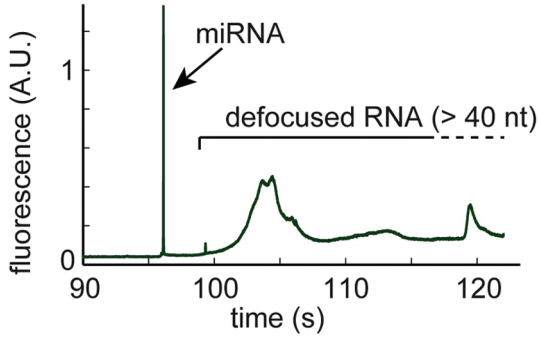

Figure 4. Typical example isotachopherogram of selective focusing of miRNA from total RNA. The sharp peak at $t = 96$ s corresponds to the ITP focused miRNA. This peak is approximately Gaussian with characteristic width around 20 ms. We attribute the peaks and plateau signal elements at larger migration times ($t > 98$ s) to defocused longer RNA molecules, which include tRNA and 5S and 5.8S rRNA. For each run, we performed a Gaussian fit on the miRNA peak and integrated signal over 3.0 standard deviations, center on the peak position. This run corresponds to a typical miRNA quantitation run for Hepa1-6 cells (5 ng·μL^{-1} in the TE).

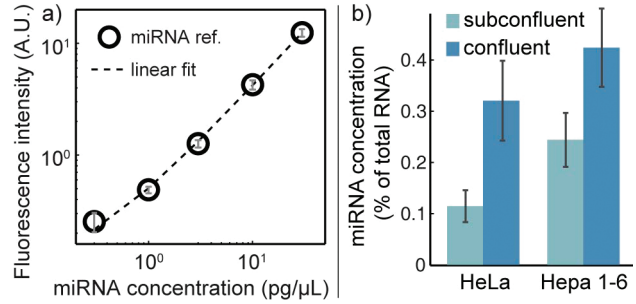

Figure 5. Calibration curve for absolute quantification of miRNA using selective ITP (a), and miRNA abundance for HeLa and Hepa1-6 subconfluent and confluent cell cultures (b). We built the calibration curve (a) by performing selective ITP of our miRNA standard at a total concentration ranging between 0.3 and 30 pg·μL^{-1}. This calibration curve is used for absolute quantitation of miRNA levels from a single fluorescence measurement. We show results of miRNA quantitation with selective ITP in (b). Shown is a comparison of miRNA levels between Hepa1-6 and HeLa cell cultures before (low density) and at confluence (high density). We diluted a total RNA in TE down to 5 ng μL^{-1} and performed the ITP assay. miRNA quantitation shows that subconfluent cells have lower miRNA expression compared to the confluent cells, consistent with the work of Hwang et al.[4] This implies that miRNA expression is not only a function of tissue type but also of tissue density. Uncertainty bars represent the 95% confidence intervals.

significant at all concentrations. In particular, at 5.5% w/v PVP, the measured (baseline) fluorescence intensity of the 40 nt RNA case was only 12% of the fluorescence of miRNA but exceeded 60% of miRNA at 4% w/v (see inset of Figure 3a). We attribute most of the residual fluorescence at 5.5% w/v to contamination (see below) and synthesis byproducts remaining after purification of the 40 mer. This titration shows refined selective focusing of miRNA with an LE2 with 5.5% w/v PVP and an RNA cutoff length between about 24 and 39 nt. The results also show that secondary structure of tRNA had no discernible effect on assay selectivity.

We explored the effect of possible miRNA base pairing on our fluorescence signal. Base pairing can strongly enhance quantum yield of typical intercalating dyes[16] and so reduces quantitation accuracy. Base pairing can occur between miRNA and its "star" sequence or with siRNA.[1] To control this, under sufficiently denaturing conditions, we performed selective focusing of the 22 nt long miR-126 and compared it to focusing of an equimolar mixture miR-126 and its perfect match. We compare these focusing experiments in Figure 3b. We measured no significant difference in fluorescence intensity between focusing of miR-126 and the associated duplex mixture. This shows our denaturing conditions are sufficient to disrupt miRNA base-pairing, thus avoiding bias in the miRNA quantitation.

For ITP with sample mixed in TE, the focused sample amount is proportional to its initial concentration.[7] Given proper calibration, the total fluorescence intensity in the ITP zone (sharp miRNA peak shown in the isotachopherogram of Figure 4) is a measurement of the initial miRNA concentration in the TE. We used an equimolar mixture of 735 synthetic miRNAs as a standard solution. This miRNA panel is widely used as an accurate reference for microarrays.[17]

We determined calibration curves by diluting the miRNA reference in the TE at relevant concentrations. We show a sample calibration curve in Figure 5a, where the miRNA concentration varied between 0.3 and 30 pg·μL^{-1}. We note that negative controls (experiments with no miRNA in the TE) yielded a reproducible fluorescent signal at the 0.1 pg·μL^{-1} level. This residual fluorescence was likely due to contamination of stock chemicals as observed routinely by us and others using ITP.[18]

To demonstrate the efficacy and utility of our assay in a strongly relevant biological application, we quantified global miRNA levels in subconfluent and confluent cell cultures.

As mentioned above, Hwang et al. showed that cell−cell contact activates miRNA biogenesis, resulting in greater miRNA abundance in densely grown cultures of various cell lines.[4] We provide further independent evidence for this effect using our ITP-based selective quantitation by measuring miRNA abundance in HeLa and Hepa1-6 cell cultures before and at confluence.

We dissolved total RNA in the TE down to 5 ng·μL^{-1} and performed miRNA quantitation with ITP as described above. We show a sample isotachopherogram in Figure 4. The sharp, early peak corresponds to the ITP zone and is nearly Gaussian in shape with approximately 10 ms detector width. The trailing defocused portion of the signal at larger migration times corresponds to longer RNA defocused within the LE2 zone. We attribute the first wide, diffused peak at 104 s (5−10 s width) to tRNA. This tRNA peak does not overlap with the focused miRNA peak and therefore does not affect quantitation. Before continuing, we note that when we performed similar measurements on degraded RNA samples, isotachopherograms showed significant tailing of the miRNA peak, a dispersed tRNA peak, and overlap between these. Degraded RNA samples also showed abnormally high levels of focused short RNA compared to higher quality preparations. Under such conditions, degraded RNA likely produced fragments shorter than the ITP cutoff length, resulting in

(16) Cosa, G.; Focsaneanu, K. S.; McLean, J. R. N.; McNamee, J. P.; Scaiano, J. C. *Photochem. Photobiol.* **2001**, *73*, 585–599.
(17) Zhang, X. X.; Graves, P. R.; Zeng, Y. *Biochim. Biophys. Acta: Gene Regul. Mech.* **2009**, *1789*, 153–159.
(18) Vreeland, W. N.; Williams, S. J.; Barron, A. E.; Sassi, A. P. *Anal. Chem.* **2003**, *75*, 3059–3065.

highly upward biased quantitation of miRNA. To avoid this bias, we systematically obtained RNA integrity numbers (RIN, measured at the Stanford PAN facility)[19] for all samples and performed measurements exclusively on samples with RIN greater than 9.0, which exceeds recommendations for miRNA analysis.[6]

We measured absolute miRNA abundance from total RNA from subconfluent and confluent cultures. We show results for HeLa and Hepa1-6 cells in Figure 5b, where the measurements are presented as a percentage of total RNA (since total RNA concentration does not vary with cell density). In both cases, we observed a significant increase in miRNA expression between the subconfluent and confluent cultures. miRNA levels increased from 0.11% to 0.32% of total RNA in HeLa cells and from 0.24% to 0.42% in Hepa1-6 cells. These results provide independent validation of the findings reported in Hwang et al.[4] and confirm the efficacy of the ITP based miRNA quantification. While relative values of miRNA levels were qualitatively similar to Hwang's study, we note that the current measurements show slightly larger concentrations of miRNA than levels estimated from microarray data.[20] We attribute this apparent discrepancy to variations of miRNA expression between different cell types and to different small RNA extraction efficiencies associated with the preparation methods.[21]

(19) Schroeder, A.; Mueller, O.; Stocker, S.; Salowsky, R.; Leiber, M.; Gassmann, M.; Lightfoot, S.; Menzel, W.; Granzow, M.; Ragg, T. *BMC Mol. Biol.* **2006**, *7*, 3.

(20) Bissels, U.; Wild, S.; Tomiuk, S.; Holste, A.; Hafner, M.; Tuschl, T.; Bosio, A. *RNA* **2009**, *15*, 2375–2384.

(21) Ach, R.; Wang, H.; Curry, B. *BMC Biotechnol.* **2008**, *8*, 69.

In summary, we have developed a new technique for accurate, fast, and absolute quantitative measurement of global miRNA levels with low sample consumption (e.g., order 10 μL volumes with 10−50 ng of total RNA) based on on-chip ITP. We demonstrated the selectivity and the accuracy of the assay and showed its utility by performing global miRNA measurements on subconfluent and confluent HeLa and Hepa1-6 cell cultures. The technique is a new, efficient tool for the investigation of the biogenesis and role of miRNAs, and its high sensitivity allows for potential application to a large variety of cells and tissues.

ACKNOWLEDGMENT

We gratefully acknowledge the support of the Defense Advanced Research Projects Agency (DARPA) and the Howard Hughes Medical Institute (HHMI). J.T.M. is a HHMI Early Career Scientist.

SUPPORTING INFORMATION AVAILABLE

Schematic of ITP and additional details on experimental methods. This material is available free of charge via the Internet at http://pubs.acs.org.

Received for review September 20, 2010. Accepted October 28, 2010.

AC102496M